


Synthesis and thermal transformation of a neodymium(III) complex $[\text{Nd}(\text{HTBA})_2(\text{C}_2\text{H}_3\text{O}_2)(\text{H}_2\text{O})_2] \cdot 2\text{H}_2\text{O}$ to non-centrosymmetric oxosulfate $\text{Nd}_2\text{O}_2\text{SO}_4$

N.N. Golovnev, M.S. Molokeevev, S.N. Vereshchagin & V.V. Atuchin


To cite this article: N.N. Golovnev, M.S. Molokeevev, S.N. Vereshchagin & V.V. Atuchin (2015) Synthesis and thermal transformation of a neodymium(III) complex $[\text{Nd}(\text{HTBA})_2(\text{C}_2\text{H}_3\text{O}_2)(\text{H}_2\text{O})_2] \cdot 2\text{H}_2\text{O}$ to non-centrosymmetric oxosulfate $\text{Nd}_2\text{O}_2\text{SO}_4$, Journal of Coordination Chemistry, 68:11, 1865-1877, DOI: [10.1080/00958972.2015.1031119](https://doi.org/10.1080/00958972.2015.1031119)


To link to this article: <https://doi.org/10.1080/00958972.2015.1031119>

 View supplementary material [↗](#)


 Published online: 11 Apr 2015.

 Submit your article to this journal [↗](#)

 Article views: 141

 View related articles [↗](#)

 View Crossmark data [↗](#)

 Citing articles: 26 View citing articles [↗](#)

Synthesis and thermal transformation of a neodymium(III) complex $[\text{Nd}(\text{HTBA})_2(\text{C}_2\text{H}_3\text{O}_2)(\text{H}_2\text{O})_2] \cdot 2\text{H}_2\text{O}$ to non-centrosymmetric oxosulfate $\text{Nd}_2\text{O}_2\text{SO}_4$

N.N. GOLOVNEV[†], M.S. MOLOKEEV*^{‡§} , S.N. VERESHCHAGIN[¶] and V.V. ATUCHIN^{||††‡‡}

[†]Department of Chemistry, Siberian Federal University, Krasnoyarsk, Russia

[‡]Laboratory of Crystal Physics, Kirensky Institute of Physics, SB RAS, Krasnoyarsk, Russia

[§]Department of Physics, Far Eastern State Transport University, Khabarovsk, Russia

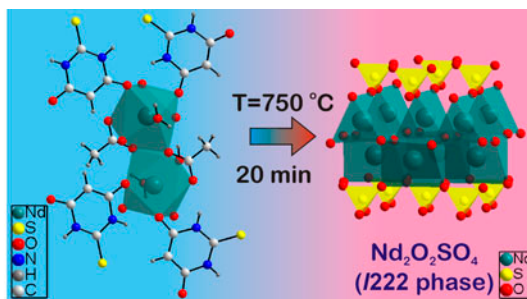
[¶]Laboratory of Catalytic Conversion of Small Molecules, Institute of Chemistry and Chemical Technology, SB RAS, Krasnoyarsk, Russia

^{||}Laboratory of Optical Materials and Structures, Institute of Semiconductor Physics, SB RAS, Novosibirsk, Russia

^{††}Functional Electronics Laboratory, Tomsk State University, Tomsk, Russia

^{‡‡}Laboratory of Semiconductor and Dielectric Materials, Novosibirsk State University, Novosibirsk, Russia

(Received 16 December 2014; accepted 2 March 2015)



Neodymium complex $[\text{Nd}(\text{HTBA})_2(\text{C}_2\text{H}_3\text{O}_2)(\text{H}_2\text{O})_2]_n \cdot 2n\text{H}_2\text{O}$ (**1**) ($\text{H}_2\text{TBA} = 2$ -thiobarbituric acid, $\text{C}_4\text{H}_4\text{N}_2\text{O}_2\text{S}$) has been synthesized in an aqueous solution at 80–90 °C. The crystal structure of **1** has been determined by the Rietveld method in space group $P2_1/n$, $a = 8.5939(2)$, $b = 22.9953(5)$, $c = 10.1832(2)$ Å, $\beta = 112.838(1)^\circ$, $Z = 4$, and $R = 0.0181$. In **1**, the Nd(III) is coordinated by four μ_2 -HTBA[−] ions through O, three oxygens from two μ_2 - η^2 : η^1 -bridging CH_3COO^- anions, and two terminal waters with a tri-capped trigonal prism structure. The prisms form an edge-contact pair through two O from two acetates. The pairs are connected by HTBA[−] and form a 3-D framework. The principle product of thermal decomposition of **1** at >750 °C is $\text{Nd}_2\text{O}_2\text{SO}_4$ (**2**). The crystal structure of **2** has been obtained in space group $I222$, $a = 4.1199(4)$, $b = 4.2233(4)$, $c = 13.3490(12)$ Å, $Z = 2$, and $R = 0.0246$. The structure is related to an orthorhombic structure type of $\text{M}_2\text{O}_2\text{SO}_4$ ($\text{M} = \text{Ln}$) compounds. In **2**, the Nd^{3+} is coordinated by six oxygens in a trigonal prism. Each NdO_6 prism links with two SO_4 tetrahedra by nodes, with four other NdO_6 prisms by edges, and with four

*Corresponding author. Email: msmolokeev@gmail.com

other NdO_6 prisms by nodes, and the units form the 3-D frame. In the frame, the layers of SO_4 tetrahedra are alternated by two NdO_6 prism layers.

Keywords: Neodymium; 2-Thiobarbituric acid; Crystal structure; Thermal decomposition; IR spectroscopy

1. Introduction

Design and synthesis of metal–organic framework compounds (MOFs) have attracted the attention in materials science because of specific molecular topologies and many potential applications [1]. 2-Thiobarbituric acid (H_2TBA) is a well-known pharmaceutical for the central nervous system [2]. Also, it is a promising ligand for MOF synthesis because it has a suitable spatial arrangement of donor atoms N, O, and S. H_2TBA can exist in several tautomeric configurations [3–11], promising for very rich MOF chemistry. Information, obtained earlier on H_2TBA coordination in metal complexes by electronic, IR, and XES spectroscopies, or magnetic measurements, yields such coordination modes as N, O, S [12–16]; N, S or N, O [17, 18]; O, N, N' [19]. However, in many cases, the proposed coordination modes need additional verification. In accordance with XRD results, when H_2TBA coordinates to metal ions of s-, p-, d- or f-block (Eu) elements, it can be connected using only oxygen [20–24], O and S [20, 21, 25–34], S [35], S and N [35, 36], or through O, S, and N [37]. There are no data, except for $([\text{Eu}_2(\text{HTBA})_6(\text{H}_2\text{O})_6]_n)_n$, concerning the crystal structures of 2-thiobarbituric acid lanthanide complexes. The bonding for lanthanide(III) complexes is noticeably different from that in the d-transition and non-transition metal complexes because lanthanide ions possess high oxophilicity and a high coordination number with values from 8 to 10. In 2-thiobarbituric complexes of Ln(III), the formation of hydrogen bonds via water, two carbonyl oxygens, two N, an S, and π – π interactions among packed thiobarbituric rings allows for building and stabilization of a high-dimensional network structure. Metal–organic frameworks based on trivalent lanthanides (LnMOFs) are a promising class of materials for addressing the challenges in engineering luminescent centers and porous compounds [1, 38, 39]. H_2TBA belongs to the chemical class of β -diketonates and complexes of rare-earth elements and β -diketonates, and LnMOFs, in particular, are of great interest due to their specific spectroscopic and magnetic properties [39–41]. Research in the field of LnMOFs is at an early stage, and comprehensive observation of the bonding effects and physical properties is topical.

In the present work, $[\text{Nd}(\text{HTBA})_2(\text{C}_2\text{H}_3\text{O}_2)(\text{H}_2\text{O})_2] \cdot 2\text{H}_2\text{O}$ (**1**) was obtained and its structure, thermal stability, and vibrational properties were characterized. The $\text{Nd}_2\text{O}_2\text{SO}_4$ (**2**) sample was obtained by thermal decomposition of **1**. Up to now, there has been no information about the $\text{Nd}_2\text{O}_2\text{SO}_4$ crystal structure. Earlier, only the crystal structures of $\text{La}_2\text{O}_2\text{SO}_4$ [42] and $\text{Eu}_2\text{O}_2\text{SO}_4$ [43] were solved. They crystallize in space group C2/c and show similar unit cell volumes of 493.11 and 445.07 Å³, respectively. This monoclinic structure could be reasonably supposed for **2**, but, experimentally, it was found that $\text{Nd}_2\text{O}_2\text{SO}_4$ should be attributed to the orthorhombic crystal system, and its structure has an I-centered cell and the twice smaller unit cell volume of 232.21 Å³ [44]. Several other contributions about oxosulfates $\text{M}_2\text{O}_2\text{SO}_4$ (M = La, Pr, Nd, Sm, Gd, Tb) [45], $\text{Gd}_2\text{O}_2\text{SO}_4$ [46], $\text{Eu}_2\text{O}_2\text{SO}_4$ [47] also show similar orthorhombic unit cells and similar XRD patterns, but the crystal structure has not been solved yet. Thus, at least two

polymorphic modifications at room temperature are possible in $M_2O_2SO_4$ ($M = La, Eu$) compounds: (i) monoclinic $C2/c$ with a big unit cell and (ii) orthorhombic I-centered cell with a smaller cell volume. Nevertheless, the crystal structure of $Nd_2O_2SO_4$ remains unknown. The physical properties of this compound, however, have been investigated to some extent due to unique luminescent and specific magnetic parameters. The $Nd_2O_2SO_4$ application in large volume oxygen storage has been proposed [48]. Besides, $Nd_2O_2SO_4$ can be used as an intermediate for Nd_2O_2S preparation [49], because the $Ln_2O_2SO_4$ treatment in a hydrogen flow results in the formation of Ln_2O_2S , efficient phosphors, and promising laser materials that could be used in electronic, X-ray medical, and other devices [50–54]. In this study, the crystal structure of the orthorhombic phase of $Nd_2O_2SO_4$ oxosulfate is solved and checked for the first time.

2. Experimental

2.1. Materials and synthesis

2-Thiobarbituric acid [CAS 504-17-6] with the purity >98% was commercially available from Fluka. Glacial acetic acid, $Nd(NO_3)_3 \cdot 6H_2O$, and sodium acetate trihydrate, all of reagent grade, were obtained from Acros and used without further purification. Glacial acetic acid (0.5 mL) was added to 0.174 g of $Nd(NO_3)_3 \cdot 6H_2O$ (0.397 mmol). The mixture was heated up to wet salt and evaporated to volume of 0.1–0.2 mL. This procedure was necessary because, as indicated by an XRD test, the $Nd(NO_3)_3 \cdot 6H_2O$ reagent contains an admixture of neodymium carbonate. After that, 4 mL of water and 0.47 g of solid sodium acetate trihydrate were added to the solution. After complete dissolution, 0.115 g of solid 2-thiobarbituric acid (0.798 mmol) was added to the solution at pH 5. The lumpy mixture was stirred and grounded, and then, it was heat-treated at 80–90 °C during 0.5 h and filtered. Final pink-violet precipitate **1** was washed using ethyl alcohol and dried in air. The residual concentrated filtrate was slowly evaporated at room temperature to achieve single crystals of **1**. The single-crystal dimensions were $0.3 \times 0.25 \times 0.05 \text{ mm}^3$, and these were suitable for X-ray structure analysis.

NdO_2SO_4 was obtained as the final thermal decomposition product of **1** heating it at 750 °C for 20 min. The pink powder agglomerates were formed in the platinum crucible used in the thermal analysis experiment described below.

2.2. Physical measurements

Simultaneous thermal analysis (STA) measurements were performed in a Netzsch STA Jupiter 449C device with Aeolos QMS 403C mass-spectrometer under dynamic argon–oxygen (20% O_2) or argon (<0.05% O_2) atmosphere at 50 mL min^{-1} total flow rate. Platinum crucibles with perforated lids were used, and the sample mass taken for STA experiments was 2–4 mg. The measurement procedure consisted of the temperature stabilization segment (30 min at 40 °C) and dynamic segment at heating rate of 10 °C min^{-1} . The qualitative composition of the evolved gasses was determined by online QMS in the multiple ion detection mode. The following predefined ions were scanned: $m/z = 18, 28, 30, 32, 43$ and $44, 45, 60, \text{ and } 64$.

2.3. Single X-ray diffraction analysis of **1**

The intensities of single crystal **1** were collected at 298 K using the SMART APEX II X-ray single crystal diffractometer (Bruker AXS) equipped with a CCD detector, graphite monochromator, and Mo K α radiation source. The unit cell of **1** corresponds to monoclinic symmetry. Space group P2₁/n was determined from the statistical analysis of the reflection intensities. The absorption corrections were applied using SADABS. The structure was solved by the direct methods using SHELXS and refined in the anisotropic approach for non-hydrogen atoms using SHELXL [55]. All hydrogens were refined in a constrained mode. In the structure, all hydrogens of HTBA⁻ and CH₃COO⁻ were positioned geometrically as riding on their parent atoms, with d(C–H) = 0.93 Å, d(N–H) = 0.86 Å, and Uiso(H) = 1.2Ueq(C, N). All water hydrogens were refined under the distance restraints of d(O–H) = 0.90(3) Å and Uiso(H) = 1.2Ueq(O).

The structure test for the presence of other missing symmetry elements and possible voids was carried out using the PLATON program [56]. A summary of the crystal data, experimental details, and refinement results are given in table 1. Selected bond lengths determined in **1** are listed in table S1 (see online supplemental material at <http://dx.doi.org/10.1080/00958972.2015.1031119>). The intermolecular hydrogen bonds in **1** are summarized in table S2. The scheme of crystal structure **1** is presented in scheme 1(a).

Table 1. The crystal structure parameters of **1** and **2**.

	1	2
Empirical formula	C ₁₀ H ₁₇ N ₄ NdO ₁₀ S ₂	Nd ₂ O ₆ S
Crystal size (mm ³)	0.3 × 0.25 × 0.05	Powder
Molecular mass	561.64	416.54
Crystal system	Monoclinic	Orthorhombic
Space group	P2 ₁ /n	I222
<i>a</i> (Å)	8.5939(2)	4.1199(4)
<i>b</i> (Å)	22.9953(5)	4.2233(4)
<i>c</i> (Å)	10.1832(2)	13.3490(12)
β (°)	112.838(1)	–
Volume (Å ³)	1854.64(7)	232.27(4)
<i>Z</i>	4	2
Diffractometer	SMART APEXII	D8 ADVANCE
Radiation type	Mo K α	Cu K α
Temperature (K)	296(2)	300
Calculated density (g cm ⁻³)	2.008	5.955
μ (mm ⁻¹)	3.083	172.54
<i>F</i> (0 0 0)	1108	368
Reflections collected	18,354	–
Independent reflections	5416	–
Data/restraints/parameters	5416/11/268	124/0/47
$2\theta_{\max}$ (°)	60.18	120
<i>h</i> , <i>k</i> , <i>l</i> - limits	–12 ≤ <i>h</i> ≤ 10; –31 ≤ <i>k</i> ≤ 32; –14 ≤ <i>l</i> ≤ 14	–
<i>R</i> _{int}	0.0273	–
Weighed refinement of <i>F</i> ²	$w = 1/[\sigma^2(F_o^2) + (0.0237P)^2 + 1.098P]$	–
Goodness-of-fit on <i>F</i> ²	1.044	–
Final <i>R</i> indices [<i>I</i> > 2σ(<i>I</i>)]	<i>R</i> ₁ = 0.0181, <i>wR</i> ₂ = 0.0488	–
<i>R</i> indices (all data)	<i>R</i> ₁ = 0.0201, <i>wR</i> ₂ = 0.0498	–
<i>R</i> _{wp} , <i>R</i> _p , <i>R</i> _{exp} , <i>R</i> _B , χ^2	–	6.65, 5.20, 5.51, 2.46, 1.21
$\Delta\rho_{\max}$ (e Å ⁻³)	0.634	–
$\Delta\rho_{\min}$ (e Å ⁻³)	–0.526	–
(Δ/σ) _{max}	0.005	–

2.4. Powder X-ray diffraction analysis

The powder X-ray diffraction data of **1** and **2** were recorded using the D8 ADVANCE (Bruker) diffractometer equipped with a VANTEC detector with a Ni filter. The measurements were performed using Cu K α radiation. The structural parameters of **1** defined by a single-crystal analysis were used as a base in Rietveld refinement of the **1** powder pattern. The refinement was produced using program TOPAS 4.2 [57]. Low *R*-factors and good refinement results, as shown in figure S1, verify the crystal structure of the powder sample to be representative of the **1** bulk structure.

The powder XRD pattern of **2** was indexed by the orthorhombic unit cell with cell parameters similar to those presented earlier [44]. As the space group and crystal structure were not suggested [32], it was decided to solve **2**. Four space groups I222, I2₁2₁2₁, Imm2, and Immm with identical hkl sets were considered for the structure. The simulated annealing process with random ion shifts in direct space was used to solve the crystal structure by TOPAS 4.2 program. Only space group I222 gave a crystal structure with the acceptable bond length values and ion coordination. The crystal structure was refined by the Rietveld method in TOPAS 4.2. The refinement was stable and gave low *R*-factors (table 1, figure S2). Checking the final structure by PLATON for the presence of other missing symmetry elements and possible voids has been performed. Selected bond lengths determined in **2** are in conventional ranges (table S1). In combination, the relations confirm the appropriate crystal structure determination. Crystal structure **2** is shown in scheme 1(b), and the atom coordinates are presented in table S3.

3. Results and discussion

3.1. Crystal structure 1

The single-crystal X-ray analysis of **1** revealed a 3-D coordination polymer crystallized in space group P2₁/n. The independent part of unit cell **1** contains one Nd³⁺, two HTBA⁻, one CH₃COO⁻, two coordinated waters, and two crystallization waters (figure 1). Each HTBA⁻

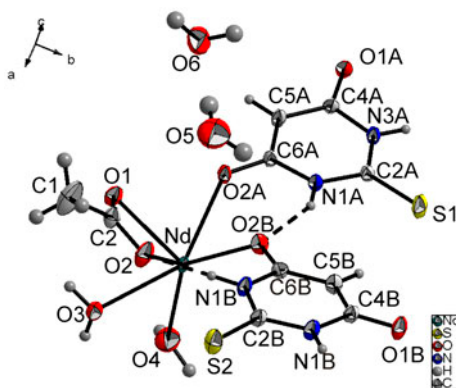


Figure 1. The independent part of the unit cell of **1**. Ellipsoids are drawn at 50% probability level and 25% probability level for crystallized water. The hydrogens are represented by spheres. The intramolecular hydrogen bonds are shown with dashed lines.

is a μ_2 -bridge linking two Nd(III) ions, and each CH_3COO^- adopts a μ_2 - $\eta^2 : \eta^1$ -bridging coordination to ligate two Nd(III) ions (scheme 1). As shown in figure 2, the Nd^{3+} is coordinated to nine oxygens, by four μ_2 -HTBA $^-$ ions, three oxygens from two CH_3COO^- anions, and two coordinated waters, in a tri-capped trigonal prism (scheme 2). The prisms are linked to each other by an edge with two oxygens from two acetates, forming a pair. The Nd_2O_{18} dimeric building blocks are formed by two NdO_9 units. The distance between Nd(III) ions in the dimeric unit is 4.2727(1) Å. These pairs have no joint nodes with other Nd polyhedrons, but they are connected to other pairs by bridged HTBA $^-$ ions and form a 3-D frame (figure 2) with 4-membered and 16-membered cycles $r(4)$ and $r(16)$. Nd–O bond lengths are 2.383(1)–2.606(2) Å, and the angle O1–Nd–O2 in the acetate anion is equal to 112.54(5)°.

There are eleven hydrogen bonds of different types N–H \cdots O, O–H \cdots O, N–H \cdots S, O–H \cdots S (table S2), forming a network where a chain along the a -axis can be marked (figure S3). The HTBA $^-$ ions in this chain form supramolecular motifs S(6) and R $_2^2$ (8), which are typical of other thiobarbiturate complexes. There are no π – π interactions between the thiobarbituric ring centers because their minimal distance is 4.048(1) Å.

3.2. Crystal structure 2

The crystal structure **2** is shown in figure 3(a). The independent part of the unit cell includes one Nd^{3+} in special position 4j, one S in 2b, and two O in 8 k and 4i positions, respectively. The S connects with four O to form a tetrahedron with the uniform bond lengths of $d(\text{S–O}) = 1.38(1)$ Å. The Nd^{3+} is coordinated by six oxygens shaped as a trigonal prism with $d(\text{Nd–O})$ values of 2.329(8)–2.380(9) Å. The NdO_6 prism is linked with two SO_4 tetrahedra by nodes, with four other NdO_6 prisms by edges, and with four other NdO_6 prisms by nodes (figure S4) so that they form a 3-D frame. In this frame, one can find alternately changed layers of SO_4 tetrahedra and two layers of NdO_6 prisms [figure 3(a)]. In the layer of NdO_6 polyhedra, there are two different prism orientations: (1) the triangle base is orthogonal to direction $\bar{a} + \bar{b}$ and (2) the base is orthogonal to direction $\bar{a} - \bar{b}$. The geometry appeared due to the equal values of the height and basic triangle side length of the NdO_6 prism.

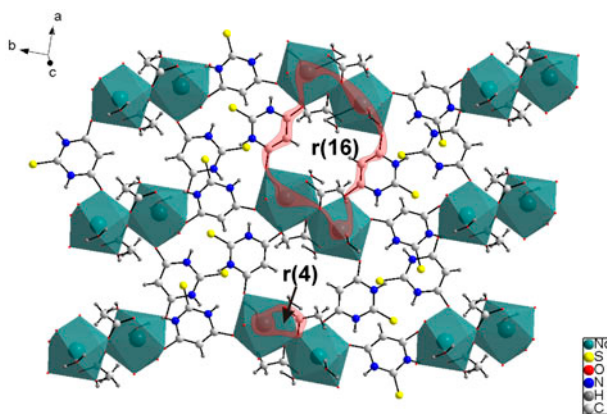


Figure 2. View of the structure of **1**. All crystallized waters are deleted to simplify. Motifs are marked by rings.

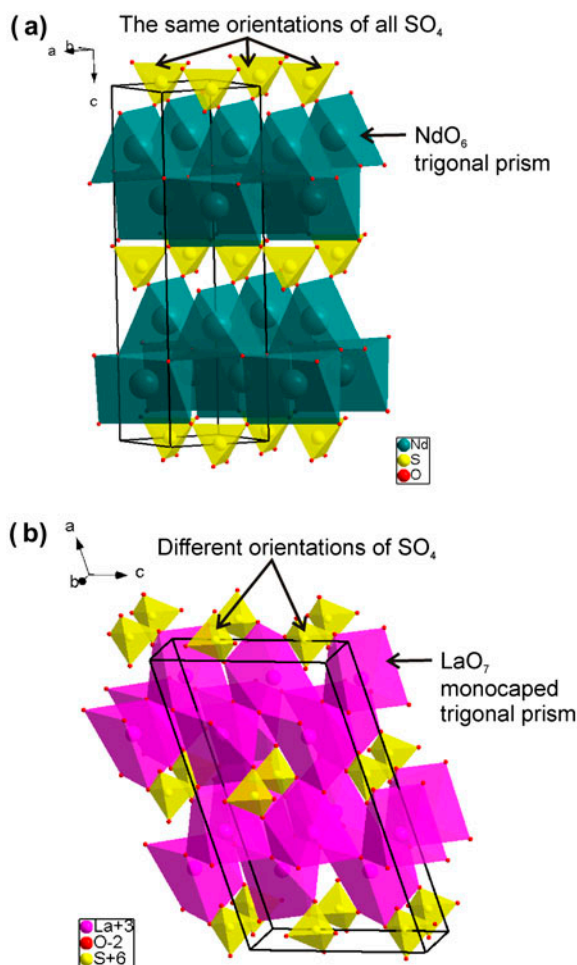


Figure 3. Comparison crystal structures of (a) orthorhombic $\text{Nd}_2\text{O}_2\text{SO}_4$ (**2**) and (b) monoclinic $\text{La}_2\text{O}_2\text{SO}_4$.

Comparison of crystal structure $\text{La}_2\text{O}_2\text{SO}_4$ ($C2/c$) [42] and $\text{Nd}_2\text{O}_2\text{SO}_4$ ($I222$) reveals at least two strong differences: (1) La^{3+} is surrounded by seven oxygens at wide ranging distances $d(\text{La}-\text{O}) = 2.253(9)–2.762(14)$ Å, forming a mono-capped trigonal prism instead of a trigonal prism and (2) SO_4 tetrahedra in monoclinic $\text{La}_2\text{O}_2\text{SO}_4$ are in two different orientations; however, in **2**, all SO_4 tetrahedra are in the same orientation [figure 3(a) and (b)]. As these crystal structures cannot be easily transformed into each other, the orthorhombic $\text{M}_2\text{O}_2\text{SO}_4$ ($M = \text{Ln}$) compounds should be attributed to a new type of crystal structure.

3.3. Thermal analysis of **1**

According to the TG–DSC data shown in figures 4 and S5, the organic moieties of **1** are thermally stable to 250 °C under oxidative and non-oxidative conditions. The thermal transformation/oxidation process of **1** may be divided into three major stages: the two

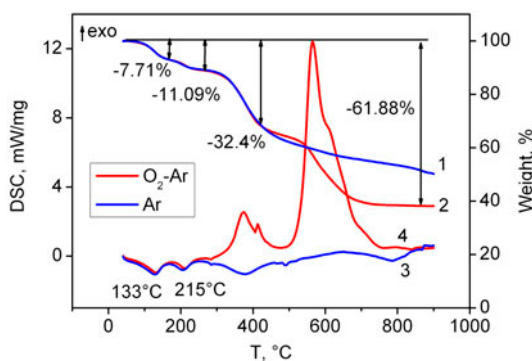
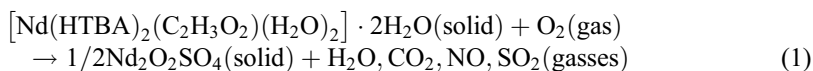


Figure 4. TG (1,2) and DSC (3,4) curves for thermal decomposition of **1** under 20%O₂-Ar (2,4) and Ar (1,3) atmospheres.

dehydration steps indicated by endothermic peaks at 133 and 215 °C (figure 4) and complex, partially resolved processes over $T = 270\text{--}900$ °C. At $T > 270$ °C, the release of CO₂, NO, SO₂ (figure S6), and H₂O relates to oxidative degradation of acetate and HTBA⁻ ions. The temperature dependences of MS curves are shown in figure S6.

The TG thermal conversion curves recorded under oxidative and non-oxidative conditions are identical at least up to 430 °C ($\Delta m = -23.4\%$). In these two cases, the thermal effects are of opposite signs, as shown in figure 4. According to the MS data shown in figure S6, the H₂O and CO₂ amounts evolved in Ar and O₂-Ar atmospheres are similar. The main difference was observed for $m/z = 60$ and 64. The $m/z = 60$ ion is probably caused by carbonyl sulfide (COS), but not by CH₃COOH, which could be expected to be formed from the acetate of **1**. This is evidenced by the absence of ions with $m/z = 43$ and 45 which are characteristic for acetic acid and simultaneous intensity enhancement of the ions with $m/z = 32$ and 60 which are characteristic for COS. COS is quickly oxidized in the presence of gas-phase oxygen within the DSC crucible, giving CO₂ and SO₂ formation and the related exo-effect in the DSC curve.

No definite product is formed after the non-oxidative calcination of **1** in Ar atmosphere. According to the XRD results, the principle product of the thermal oxidation of **1** is Nd₂O₂SO₄. The theoretical mass loss Δm_{Calcd} for **1**, according to equation (1), is 62.92%, slightly different from the experimentally observed value of $\Delta m_{\text{exp}} = 61.88\%$. The probable reason is the partial loss of lattice water from the sample under a dry O₂-Ar flow during the temperature stabilization stage of the measurement procedure.



An independent estimation of water content in **1**, directly in the STA unit, may be based on the mass spectral intensity of the ions with $m/z = 18$ (H₂O⁺) which is proportional to the sum of the lattice water, coordinated water, and H₂O formed from the acetate and HTBA moieties oxidation. Using the integral H₂O⁺ ion intensity from 40 to 270 °C and from 40 to 900 °C (figure S6, curve 3), the water content in **1** was determined to be at the level of 3.4 H₂O molecule per complex molecule.

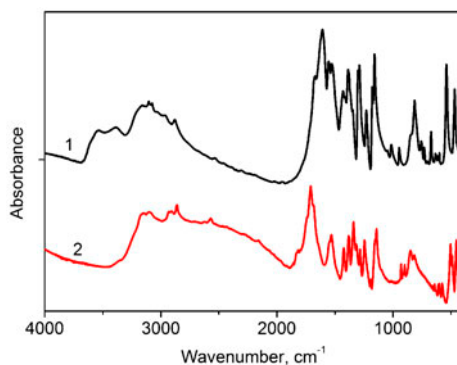


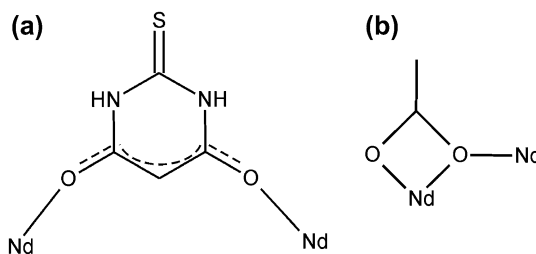
Figure 5. IR spectra of $[\text{Nd}(\text{HTBA})_2(\text{C}_2\text{H}_3\text{O}_2)(\text{H}_2\text{O})_2]\cdot 2\text{H}_2\text{O}$ (**1**) and **III** polymorph modification of 2-thiobarbituric acid (**2**).

The supposed sequence of $[\text{Nd}(\text{HTBA})_2(\text{C}_2\text{H}_3\text{O}_2)(\text{H}_2\text{O})_2]\cdot 1.4\text{H}_2\text{O}$ transformations on heating is depicted in scheme 3. The first stage of the dehydration results in lattice water elimination and partial coordinated water loss to form the monohydrate, which, in turn, is dehydrated to anhydrous $[\text{Nd}(\text{HTBA})_2(\text{C}_2\text{H}_3\text{O}_2)]$. Experimental mass losses Δm_{exp} are sufficiently close to the theoretical values of Δm_{clc} , both for the dehydration stages and the total conversion to $\text{Nd}_2\text{O}_2\text{SO}_4$.

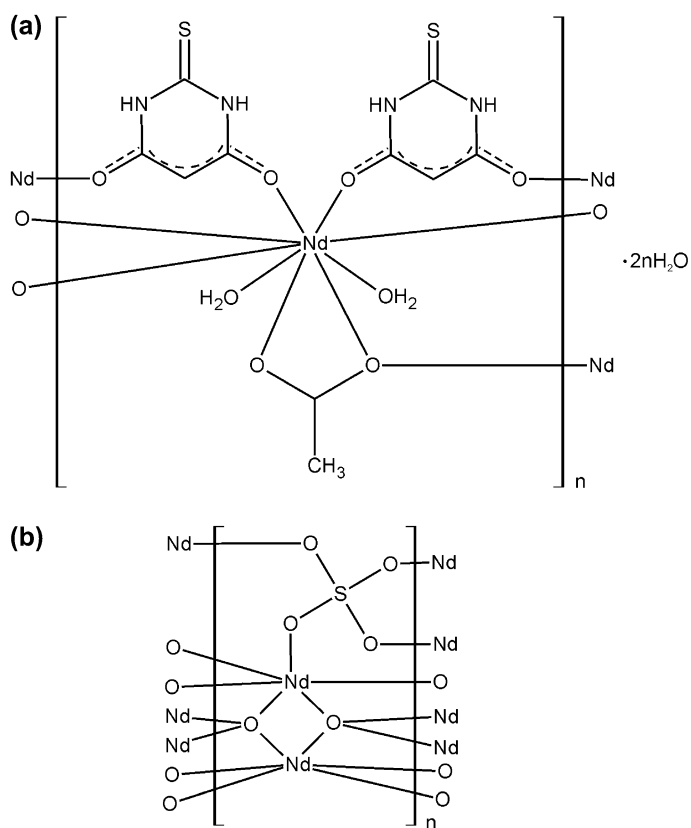
3.4. IR absorption spectrum of **1**

The following bands were found in the IR absorption spectrum of **1** shown in figure 5, curve 1 (cm^{-1}): 3537 w., 3388 w., 3104 m., 3076 m., 2880 w., 1674 s., 1610 vs., 1558 s., 1430 m., 1387 s., 1301 s., 1289 s., 1230 m., 1164 vs., 1015 w., 946 w., 814 m., 756 w., 730 w., 705 vw., 671w., 634 vw., 623 vw., 608 vw., 600 vw., 539 s., 464 s., and 419 v. (vs. – very strong, s. – strong, m. – medium, w. – weak, and vw. – very weak). For comparison, the IR spectrum of **III** polymorph modification of 2-thiobarbituric acid is shown in figure 5, curve 2 [58].

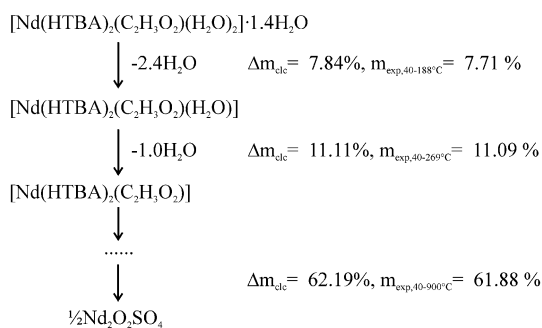
The presence of the two ligands containing a carbonyl group in **1** hinders specific assignment of the bands $\nu(\text{C}=\text{O})$ observed in IR spectra (figure 5). According to earlier results [3, 8, 10, 11, 53], the high intensity bands at $1387\text{--}1674\text{ cm}^{-1}$ can be attributed to $\nu(\text{C}=\text{O})$ vibrations. The high intensity bands at 1684 and 1708 cm^{-1} , as observed in **III**



Scheme 1. Coordination modes of HTBA^- and CH_3COO^- anions in the structure of **1**.



Scheme 2. Structure of (a) $[\text{Nd}(\text{HTBA})_2(\text{C}_2\text{H}_3\text{O}_2)(\text{H}_2\text{O})_2] \cdot 2\text{H}_2\text{O}$ (1); (b) $\text{Nd}_2\text{O}_2\text{SO}_4$ (2).



Scheme 3. The transformation sequence of 1.

H_2TBA , are not detected in the IR spectrum of **1**. Also, there is a difference between the wave number positions of $\nu(\text{C}=\text{O})$ bands at $1380\text{--}1610\text{ cm}^{-1}$ for **1** and H_2TBA . The data indicate the coordination of the ligand through the oxygen. The strong band at 1155 cm^{-1} in the IR spectrum of H_2TBA , which is attributed to $\nu(\text{C}=\text{S})$ [3, 10, 59], is also observed in

the IR spectrum of **1**, and this is consistent with the absence of ligand coordination through the donor sulfur. Therefore, the results of IR spectroscopy are consistent with X-ray data.

4. Conclusion

A new $[\text{Nd}(\text{HTBA})_2(\text{C}_2\text{H}_3\text{O}_2)(\text{H}_2\text{O})_2]_n \cdot 2n\text{H}_2\text{O}$ (**1**) and $\text{Nd}_2\text{O}_2\text{SO}_4$ (**2**) were prepared. Structure **1** is a 3D MOF and **2** is an inorganic 3D polymer. Complex **1** is thermally stable in the air at least up to 100 °C and transforms into **2** at $T > 750$ °C. The final **2** is of high phase purity and thermal decomposition of $[\text{Ln}(\text{HTBA})_2(\text{C}_2\text{H}_3\text{O}_2)(\text{H}_2\text{O})_2]_n \cdot 2n\text{H}_2\text{O}$ could be proposed as an efficient route for the synthesis of $\text{Ln}_2\text{O}_2\text{SO}_4$ compounds. However, monoclinic and orthorhombic structures currently reported for different $\text{Ln}_2\text{O}_2\text{SO}_4$ compounds, and thermal ranges of the existence of modification are unclear. Thus, it would be interesting to try the synthesis of the known monoclinic modification, for example, $\text{La}_2\text{O}_2\text{SO}_4$ or $\text{Eu}_2\text{O}_2\text{SO}_4$, through the $[\text{Ln}(\text{HTBA})_2(\text{C}_2\text{H}_3\text{O}_2)(\text{H}_2\text{O})_2]_n \cdot 2n\text{H}_2\text{O}$ decomposition route. This may be of practical significance because $\text{Ln}_2\text{O}_2\text{SO}_4$ oxosulfates are precursors of $\text{Ln}_2\text{O}_2\text{S}$ which are efficient phosphors used in many devices.

Supplementary material

Crystallographic data (excluding structure factors) for the structural analysis of **1** have been deposited with the Cambridge Crystallographic Data Center, No. CCDC-1031120. Copies may be obtained free of charge from the Director, CCDC, 12 Union Road, Cambridge CB2 1EZ, UK (Fax: +44 (1223) 336-033, E-mail: deposit@ccdc.cam.ac.uk, or [www: http://www.ccdc.cam.ac.uk](http://www.ccdc.cam.ac.uk)).

Further details of crystal structure **2** may be obtained from Fachinformationszentrum Karlsruhe, 76344 Eggenstein-Leopoldshafen, Germany (Fax: (+49) 7247-808-666; E-mail: crystdata@fiz-karlsruhe.de; http://www.fiz-karlsruhe.de/request_for_deposited_data.html on quoting the deposition number CSD-428672).

Acknowledgments

The study was carried out within the public task of the Ministry of Education and Science of the Russian Federation for research engineering at the Siberian Federal University in 2014. V.V.A. is grateful to the Ministry of Education and Science of the Russian Federation for the financial support of this investigation.

Disclosure statement

No potential conflict of interest was reported by the authors.

ORCID

M.S. Molochev  <http://orcid.org/0000-0002-8297-0945>

References

- [1] H.-C. Zhou, J.R. Long, O.M. Yaghi. *Chem. Rev.*, **112**, 673 (2012).
- [2] S. Bondock, A. El-Gaber Tarhoni, A.A. Fadda. *Phosphorus, Sulfur Silicon Relat. Elem.*, **182**, 1915 (2007).
- [3] B.A. Ivin, V.I. Slesarev, N.A. Smorygo. *Russ. J. Org. Chem.*, **10**, 1968 (1974).
- [4] B.A. Ivin, V.I. Slesarev. *Russ. J. Org. Chem.*, **10**, 113 (1974).
- [5] M.S. Jovanovic, E.R. Biehl. *J. Heterocycl. Chem.*, **24**, 191 (1987).
- [6] S. Millefiori, A. Millefiori. *J. Heterocycl. Chem.*, **26**, 639 (1989).
- [7] S. Stoyanov, I. Petkov, L. Antonov, T. Stoyanova. *Can. J. Chem.*, **68**, 1482 (1990).
- [8] F. Ramondo, A. Pieretti, L. Gontrani, L. Bencivenni. *Chem. Phys.*, **271**, 293 (2001).
- [9] F. Zuccarello, G. Buemi, C. Gandolfo, A. Contino. *Spectrochim. Acta, Part A*, **59**, 139 (2003).
- [10] E. Méndez, M.F. Cerdá, J.S. Gancheff, J. Torres, C. Kremer, J. Castiglioni, M. Kieninger, O.N. Ventura. *J. Phys. Chem. C*, **111**, 3369 (2007).
- [11] R.I. Bakalska, V.B. Delchev. *Acta Chim. Slov.*, **59**, 75 (2012).
- [12] M.S. Masoud, A.M. Heiba, F.M. Ashmawy. *Transition Met. Chem.*, **8**, 124 (1983).
- [13] L. Palomino, B.E. Zaitcev, R.K. Gridasova, T.M. Ivanova. *Russ. J. Inorg. Chem.*, **33**, 2347 (1988).
- [14] L. Palomino, B.E. Zaitcev, T.M. Ivanova, P.I. Abramenko. *Russ. J. Inorg. Chem.*, **34**, 2901 (1989).
- [15] Z.M. Zaki, G.G. Mohamed. *Spectrochim. Acta, Part A*, **56**, 1245 (2000).
- [16] M.S. Refat, S.A. El-Korashy, A.S. Ahmed. *Spectrochim. Acta, Part A*, **71**, 1084 (2008).
- [17] A. Jiménez, H. Jiménez, J. Borrás. *Synth. React. Inorg. Met.-Org. Chem.*, **17**, 159 (1987).
- [18] M.S. Masoud, S.S. Haggag, E.A. Khalil. *Nucleos. Nucleot. Nucleic Acids*, **25**, 73 (2006).
- [19] K.S. Siddiqi, P. Khan, S. Khan, S.A. Zaidi. *Synth. React. Inorg. Met.-Org. Chem.*, **12**, 681 (1982).
- [20] N. Golovnev, M. Molokeev. *Acta Crystallogr., Sect. C: Cryst. Struct. Commun.*, **69**, 704 (2013).
- [21] N.N. Golovnev, M.S. Molokeev, S.N. Vereshchagin, V.V. Atuchin. *J. Coord. Chem.*, **66**, 4119 (2013).
- [22] Z.R. Pan, Y.C. Zhang, Y.L. Song, X. Zhuo, Y.Z. Li, H.G. Zheng. *J. Coord. Chem.*, **61**, 3189 (2008).
- [23] N.N. Golovnev, M.S. Molokeev. *Russ. J. Coord. Chem.*, **40**, 648 (2014).
- [24] B. Li, W. Li, L. Ye, G.-F. Hou, L.-X. Wu. *Acta Crystallogr., Sect. E: Struct. Rep. Online*, **66**, m1546 (2010).
- [25] N.N. Golovnev, M.S. Molokeev. *Russ. J. Inorg. Chem.*, **58**, 1193 (2013).
- [26] N.N. Golovnev, M.S. Molokeev. *J. Struct. Chem.*, **54**, 968 (2013).
- [27] V.I. Balas, I.I. Verginadis, G.D. Geromichalos, N. Kourkoumelis, L. Male, M.B. Hursthouse, K.H. Repana, E. Yiannaki, K. Charalabopoulos, T. Bakas, S.K. Hadjidakou. *Eur. J. Med. Chem.*, **46**, 2835 (2011).
- [28] N.N. Golovnev, M.S. Molokeev, M.Y. Belash. *J. Struct. Chem.*, **54**, 566 (2013).
- [29] N.N. Golovnev, M.S. Molokeev, S.N. Vereshchagin, V.V. Atuchin, M.Y. Sidorenko, M.S. Dmitrushkov. *Polyhedron*, **70**, 71 (2014).
- [30] M. Kubicki, A. Owczarzak, V.I. Balas, S.K. Hadjidakou. *J. Coord. Chem.*, **65**, 1107 (2012).
- [31] N.N. Golovnev, M.S. Molokeev. *Russ. J. Inorg. Chem.*, **59**, 72 (2014).
- [32] Y. Gong, Z. Hao, J.-H. Li, T. Wu, J.-H. Lin. *Dalton Trans.*, **42**, 6489 (2013).
- [33] N.N. Golovnev, M.S. Molokeev. *Russ. J. Inorg. Chem.*, **59**, 943 (2014).
- [34] N.N. Golovnev, M.S. Molokeev. *J. Struct. Chem.*, **55**, 912 (2014).
- [35] W.J. Hunks, M.C. Jennings, R.J. Puddephatt. *Inorg. Chem.*, **41**, 4590 (2002).
- [36] K. Yamanari, M. Kida, A. Fuyuhiko, M. Kita, S. Kaizaki. *Inorg. Chim. Acta*, **332**, 115 (2002).
- [37] N.N. Golovnev, M.S. Molokeev. *J. Struct. Chem.*, **55**, 125 (2014).
- [38] J. Kido, Y. Okamoto. *Chem. Rev.*, **102**, 2357 (2002).
- [39] J. Rocha, L.D. Carlos, F.A. Almeida Paz, D. Ananias. *Chem. Soc. Rev.*, **40**, 926 (2011).
- [40] S.-D. Jiang, S.-S. Liu, L.-N. Zhou, B.-W. Wang, Z.-M. Wang, S. Gao. *Inorg. Chem.*, **51**, 3079 (2012).
- [41] H.L.C. Feltham, S. Brooker. *Coord. Chem. Rev.*, **276**, 1 (2014).
- [42] S.G. Zhukov, A. Yatsenko, V.V. Chernyshev, V. Trunov, E. Tserkovnaya, O. Antson, J. Hölsä, P. Baulés, H. Schenk. *Mater. Res. Bull.*, **32**, 43 (1997).
- [43] I. Hartenbach, T. Schleid. *Z. Anorg. Allg. Chem.*, **628**, 2171 (2002).
- [44] M. Skrobjan, N. Sato, M. Saito, T. Fujino. *J. Alloys Compd.*, **210**, 291 (1994).
- [45] V. Laptev, Yu Suponitskii, A. Vorob'ev. *Russ. J. Inorg. Chem.*, **32**, 305 (1987).
- [46] B.J. Haynes. *J. Electrochem. Soc.*, **115**, 1060 (1968).
- [47] M. Karppinen, M. Leskelä, L. Niinistö. *J. Therm. Anal.*, **35**, 355 (1989).
- [48] X.-H. Liu, D. Zhang, J.-H. Jiang, N. Zhang, R.-Z. Ma, H.-B. Zeng, B.-P. Jia, S.-B. Zhang, G.-Z. Qiu. *RSC Advances*, **2**, 9362 (2012).
- [49] P.O. Andreev, E.I. Sal'nikova, A.A. Kislitsyn. *Russ. J. Phys. Chem. A*, **87**, 1482 (2013).
- [50] YuV Orlovskii, T.T. Basiev, K.K. Pukhov, M.V. Polyachenkova, P.P. Fedorov, O.K. Alimov, E.I. Gorokhova, V.A. Demidenko, O.A. Khristich, R.M. Zakalyukin. *J. Lumin.*, **125**, 201 (2007).
- [51] G. Blasse. *Luminescent Materials*, p. 219, Springer, Berlin (1994).
- [52] M. Chertanov, O.K. Moune, B. Piriou, J. Dexpert-Ghys, M. Faucher, M. Guittard. *J. Lumin.*, **59**, 231 (1994).
- [53] C. Cui, G. Jiang, P. Huang, L. Wang, D. Liu. *Ceram. Int.*, **40**, 4725 (2014).
- [54] J. Llanos, V. Sánchez, C. Mujica, A. Buljan. *Mater. Res. Bull.*, **37**, 2285 (2002).
- [55] G.M. Sheldrick. *Acta Crystallogr., Sect. A: Found. Crystallogr.*, **64**, 112 (2008).

- [56] *PLATON – A Multipurpose Crystallographic Tool*, Utrecht University, Utrecht, The Netherlands (2008).
- [57] Bruker AXS *TOPAS V4: General Profile and Structure Analysis Software for Powder Diffraction Data – User's Manual*, Bruker AXS, Karlsruhe, Germany (2008).
- [58] N.N. Golovnev, M.S. Molokeev, L.S. Tarasova, V.V. Atuchin, N.I. Vladimirova. *J. Mol. Struct.*, **1068**, 216 (2014).
- [59] N.A. Smorygo, B.A. Ivin. *Khim. Geterotsykl. Soedin.*, **10**, 1402 (1975).